Journal of Applied Polymer Science

Microfiltration membranes functionalized with multiple styrenic homopolymer and block copolymer grafts

Jayraj K. Shethji, Stephen M. C. Ritchie
Department of Chemical and Biological Engineering, The University of Alabama, Tuscaloosa, Alabama 35401
Correspondence to: S. M. C. Ritchie (E-mail: sritchie@eng.ua.edu)

ABSTRACT: The pores of microfiltration polyethersulfone membranes have been functionalized with homopolymer and block copolymer grafts through sequential cationic polymerization of styrene and substituted styrene monomers, namely 4-chloromethylstyrene and 4-ethoxystyrene. ^{1}H NMR characterization confirmed successful incorporation of polymeric grafts at different stages of functionalization. The functionalized membrane showed a 90% decrease in membrane permeability compared to the raw membrane indicating the presence of polymeric chains in the membrane flow path. Functionalized membranes have as many as 125 repeat units per chain equating to an ion-exchange capacity (IEC) of 4.9 meq/g, representing 92% of the theoretical IEC of an ion-exchange resin. A pseudo-first-order kinetic equation correlated well ($R^2 \sim 0.99$) with the experimental kinetic data of formation of polymeric grafts. Polymer growth studies showed that at lower initiator surface density (initiator contact time <135 min), graft length and IEC were impacted by monomer feed concentration and initiator contact time. © 2015 Wiley Periodicals, Inc. J. Appl. Polym. Sci. **2015**, *132*, 42501.

KEYWORDS: copolymers; functionalization of polymers; grafting; membranes

Received 25 March 2015; accepted 15 May 2015
DOI: 10.1002/app.42501

INTRODUCTION

Microfiltration (pore size 0.1–1 μm) membranes work on the principle of size exclusion, filtering larger molecules and allowing the smaller molecules to pass through the membrane. These membranes are typically used in separation of bacteria and viruses from water, filtration of suspended solids (fruit juices, wines, and insoluble solids in industrial water), and separation of oil–water emulsions.[1–6] However, by altering the surface chemistry or by incorporating functional groups in the pores of the membrane, these materials have the potential for versatile applications including but not limited to high capacity (0.3–3.7 mg metal/cm^2 membrane area) metal capture and advanced bioseparations.[7–14] These membranes are called functionalized membranes and allow selective separations based on driving forces such as physical and chemical interactions and charge due to incorporation of ionizable functionalities in the membrane substrate.[7,10,15] Functional groups or moieties are attached to the internal pore surface as opposed to external surface of membrane which represents only 0.1% of the total available area.[16] This allows incorporation of a large number of active sites; in addition, the wide pore structure allows easy access of sites to the target molecules. Membranes functionalized with sulfonated polystyrene grafts within the pores have potential for applications in acid catalysis and separation of whey proteins.[16–18] These membranes have as many as 100 average number of repeat units per chain indicating the presence of large number of active sites.[16]

Functionalization of the microfiltration membrane can be accomplished either by polymerization *in-situ* or by grafting large-chain polymers on the polymeric backbone.[7,16–21] Polymeric membrane substrates, such as cellulosics, polysulfones, polycarbonates, polyolefins, and polyacrylates, have been functionalized by activation of pore surface.[7,9,21–25] Functional groups can be incorporated by a variety of functionalization techniques including: radiation-induced (UV radiation, γ-radiation, or electron beam) grafting, plasma-induced grafting, and chemical grafting.[16,17,26–30] Problems with radiation-induced grafting include the expensive radiation source and associated hazards, alteration of intrinsic membrane properties, e.g., solubility and stability of the substrate material, nonuniform distribution of active sites, requirements for specialized equipment, and membrane degradation.[31] The advantage of plasma-induced grafting is that it is a simple one-step process and does not alter the properties of the substrate. However, the process involves electron-induced excitation, and ionization and dissociation because of which electrons and ions react with the monomer and the polymeric substrate through undesirable side reactions.[19,29] This results in difficulties in membrane characterization due to formation of active sites with a wide variety of surface chemistries and functionalities.[32]

Chemical grafting proceeds via free radical or ionic (anionic and cationic) grafting. One of the drawbacks of free radical polymerization (FRP) is the formation of polydisperse polymers with broad molar mass distribution due to chain transfer and automatic termination reactions.[33] Atom transfer free radical polymerization (ATRP) is the controlled/living polymerization technique that addresses the limitations of FRP by synthesizing polymers with narrow molecular weight distribution and end functional groups.[34–37] Linear and branched polymer layers with controlled architecture have been successfully grafted in the pore walls of poly(ethylene terephthalate) track-etched membranes by the ATRP technique.[38,39] However, the known disadvantage of the ATRP technique is the contamination of the polymer matrix by the transition-metal catalyst used to control polymerization, e.g., copper halide.[40,41] Functional monomers have also been successfully grafted through anionic living polymerization.[42,43]

In this research, controlled/living sequential cationic polymerization technique is used for synthesis of the functionalized membrane. The proton from the acid is transferred to the monomer to form a carbocation. The propagation reaction occurs by electrophilic addition of the monomer to the growing carbocation. Thus, the advantage of cationic polymerization is that it is a living polymerization and is only limited by the availability of monomer. Additionally, monomers can be added sequentially while minimizing side reactions, termination, and chain transfer. This gives the opportunity to create well-defined block copolymers in different stages by using a different monomer at each stage, and therefore, a highly customized graft can be synthesized. Furthermore, as compared to anion living polymerization, carbocations are more reactive than carboanions and chain transfer reactions are too slow as compared to propagation reactions. Therefore, polymers with more controlled and narrow molecular weight distribution can be synthesized.[44]

The focus of this article is to synthesize and characterize a functionalized membrane by sequential cationic polymerization of styrene and substituted styrene monomers like 4-ethoxystyrene (ES) and 4-chloromethylstyrene (CMS) using sulfuric acid as an initiator. The monomers used will result in incorporation of active sites with different functional groups like sulfonic acid, phenyl, ethoxy, and chloromethyl in the pores of MF PES membrane. The research objectives include synthesis of homopolymer and block copolymer grafts, kinetic study of polymer growth, determination of membrane properties like permeability, ion-exchange capacity (IEC), and graft length and understanding controlled polymer growth. One of the unique aspects of this work is membrane pore functionalization using different monomers by living cationic polymerization.

EXPERIMENTAL

Materials

MF PES membranes were purchased from Millipore Corporation, Bedford, MA. Membrane properties include an average pore size of 0.22 μm, a thickness of 165 μm, and a diameter of 47 mm. Sulfuric acid solutions of 0.5 N were prepared from 99% sulfuric acid and distilled water. Base solutions of 0.1 N NaOH were prepared from 1 N NaOH solution by dilution with distilled water. Styrene, CMS, and ES were used for polymerization and formation of block copolymers. All the monomers were stored at 5°C until needed. Laboratory grade toluene was used as a solvent since it is soluble with styrene, ES, and CMS. Laboratory-grade methanol was used as the sample diluter for analysis of styrene-toluene and CMS-toluene permeate solutions by UV–visible spectroscopy. Deuterated dimethylsulfoxide-d_6 (DMSO) and deuterated chloroform ($CDCl_3$) were used as solvents for ^{1}H NMR analysis. All chemicals and solvents were obtained from Fisher Scientific (Pittsburgh, PA) or VWR (West Chester, PA) unless otherwise stated. The solvents were used as received without further purification, except where noted.

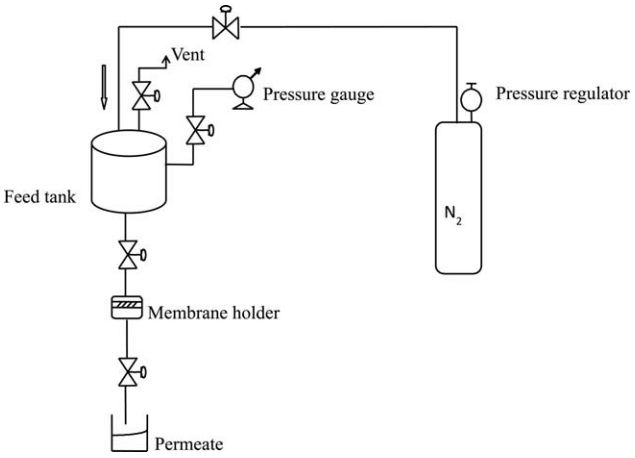

Figure 1. Schematic of the experimental laboratory setup.

Experimental Setup

The membranes used in this research were prepared by a simple, three-step procedure. First, the initiator using 0.5 N sulfuric acid was immobilized in the pores of membrane, a solution of styrene in toluene was permeated to create a homopolymer graft structure and this is followed by permeation of CMS or ES to form diblock copolymer grafts. Figure 1 shows a schematic of the customized experimental laboratory setup. The first step was to wash the whole apparatus with distilled water. This was done by flushing distilled water from the top of the tank and allowing the water to flow through the membrane holder by keeping the valves (upstream and downstream of membrane holder) open. The pH of the water collected from bottom is checked and the apparatus was washed until the pH reaches 7. The microfiltration membrane, in the form of white circular disc, was kept in a versatile stainless-steel membrane holder. The valves upstream and downstream of membrane holder were closed and the reaction solutions were fed into the carbon steel feed cell. The feed tank was then pressurized with pure nitrogen (zero grade to prevent contamination) at 21 psig and kept constant with a regulator on the nitrogen cylinder. The tank pressure is indicated by a pressure gauge attached at the top of the tank. Next, the valves are opened to allow the reaction solutions to permeate through the membrane. Permeate is collected at atmospheric pressure from the bottom. All experiments were performed at room temperature. It should be noted that since the membrane is microfiltration with large pore size, the flow

rate of solution through the membrane is very high. Hence, a valve downstream of membrane holder was kept half open to maintain a flow of 1 mL/min. Additionally, pure water flux was measured after each stage of modification to quantify changes in permeability.

Membrane Preparation

Initiator Immobilization. The feed tank was filled with 250 mL of 0.5 N H_2SO_4 and the solution was permeated through the membrane for 3 h. After permeation, the membrane was taken out of the membrane holder and rinsed multiple times with distilled water until the water pH reached 7. The membrane was then dried in air (~2 h) until the mass was constant. The apparatus was washed with distilled water after acid treatment and allowed to dry.

Synthesis of Homopolymer Grafts. Styrene, ES, and CMS monomers were used to create homopolymer grafts by treating the sulfonated membrane with the desired monomer. The sulfonated membrane was wetted with pure toluene for a few seconds and immediately placed in the membrane holder prior to the polymerization step to prevent membrane cracking. For each monomer, a 5 vol % solution of monomer in toluene was permeated at constant pressure drop of 21 psi across the membrane for 120 min. For example, 100 mL (5 mL styrene + 95 mL toluene) of styrene/toluene solution was permeated with recycle through the membrane to synthesize polystyrene grafts. Similar solutions were used to synthesize polychloromethylstyrene (100 mL total) and polyethoxystyrene (25 mL total) homopolymer grafts. In each case, the permeate was collected from the bottom and the volume was measured. The membrane was washed with pure toluene by permeating toluene through the membrane to remove the unreacted styrene. Unreacted styrene in the toluene was measured by UV–visible spectroscopy at the characteristic peak wavelength of 291 nm using methanol as a solvent.

Synthesis of Block Copolymer Grafts in the Membrane Matrix. Block copolymers were formed by polymerization of styrene, followed by sequential polymerization with CMS or ES to synthesize block copolymer grafts of poly(styrene-b-CMS) or poly(styrene-b-ES), respectively. After styrene polymerization, the feed tank was washed thoroughly with toluene to remove residual styrene (~2 washes). Next, the block copolymer was formed by permeating a 5 vol % monomer solution for either CMS or ES. As in the previous section, CMS/toluene solution (100 mL total) or ES/toluene solution (25 mL total) was permeated through the polymerized membrane at a constant pressure drop of 21 psi for 120 min. The permeate was collected and the volume was measured. The membrane was allowed to dry in air and the mass of the membrane was measured.

Analytical Procedure

Membrane Permeability Measurements. The feed tank, membrane holder, and connecting pipes, as shown in Figure 1, were rinsed with distilled water. The feed tank was next filled with distilled water. The membrane was placed into the membrane holder. The valves upstream and downstream of membrane holder were closed. The tank was then pressurized by adjusting the pressure to 5 psig using the pressure regulator on the nitrogen cylinder. The valves were then opened and the system was allowed to come to steady state (~5 min) until the flow rate was constant. The permeate was collected at 2-min intervals and three readings were taken. The process was repeated with a full tank at incremental pressures of 10, 15, 20, 25, and 30 psig.

^{1}H NMR Characterization. The compositions of homopolymers and block copolymers were characterized by ^{1}H NMR. ^{1}H NMR spectra were recorded using Bruker spectrometer operating at a resonance frequency of 600 MHz. Dimethylsulfoxide (20 mL) and deuterated chloroform (10 mL) were used as solvents. Raw and modified membranes were dissolved in solvents (~30 min) and 0.8 mL of sample was used in NMR tube to generate each spectrum.

Atomic Absorption Spectroscopy. The IECs of the raw and functionalized membranes were quantified by elemental analysis of regenerated sodium ions ($\lambda = 589$ nm) in sulfuric acid solution using atomic absorption spectroscopy (Varian 220 FS). In each case, the membrane was treated with 0.1 N NaOH (100 mL) by convection for approximately 180 min at a pressure drop of 21 psi. The membrane was then rinsed with deionized water to remove any nonspecifically bound sodium in the membrane pores. Finally, the membrane was retreated with 0.5 N H_2SO_4 (250 mL) for 180 min to regenerate sodium ions from the pores. IEC capacity is calculated as total milliequivalents of sodium ions available for exchange per gram dry weight of sulfonated membrane.

UV–Visible Spectroscopy Analysis. Samples of styrene/toluene and CMS/toluene were diluted at 1 : 1250 and 1 : 416, respectively, with pure methanol. Styrene and CMS monomer concentrations were quantified in the feed and permeate samples after polymerization by UV–visible spectrophotometry at characteristic peak wavelengths of 291 and 295 nm, respectively. The characteristic peak wavelength of toluene was at 281 nm, so there was no interference. Spectral data was obtained using a Shimadzu UV-2401 spectrophotometer.

Gas Chromatography Analysis. Samples of ES-toluene were diluted 1 : 1 with pure methanol. ES concentrations were determined in the feed and permeate solutions using gas chromatography at an elution time of 1.56 min. The elution times of methanol and toluene were 0.1 and 0.2 min, respectively, so there were no interferences. All reaction samples were analyzed using a Shimadzu GC-14A gas chromatograph equipped with a flame ionization detector. A 30 m × 0.53 mm i.d. capillary column (Rtx-624, Restek Corporation) containing a 6% cyanopropylphenyl and 94% dimethyl polysiloxane-based stationary phase was used for analysis. Helium (470 kPa) was used as the carrier gas. Hydrogen (110 kPa) and compressed air (120 kPa) gases were used to ignite the flame. The GC range was kept at 3 in order to avoid flat top peaks and to ensure good resolution. The oven temperature was kept constant at 125°C and sample run time was 5 min.

RESULTS AND DISCUSSION

Membrane Permeability Studies

Permeability studies were carried out in a batch mode. A flat sheet membrane disc made from PES was used in all experiments. The PES membranes were sealed with a 4.1 cm inner

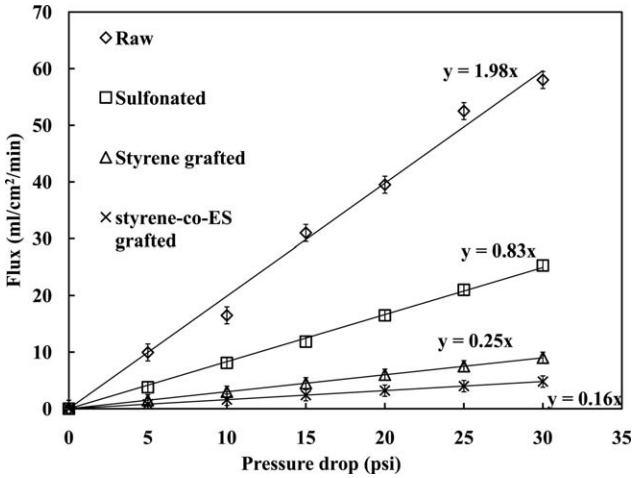

Figure 2. Polymer growth effect on membrane permeability.

diameter o-ring. Therefore, 4.1 cm was considered as the membrane effective diameter for calculating the flux. The membrane effective area was 13.2 cm^2. Pure water permeation flux is directly proportional to pressure drop, and the slope of the straight line gives the membrane permeability.

Permeability studies were carried out on raw, sulfonated, polystyrene, poly(styrene-b-ES), and poly(styrene-b-CMS)-grafted membranes to compare the effects of polymer graft formation on membrane flux. Polymer growth in the pores of the membrane should reduce the effective pore size in each case, and therefore, a decrease in permeability was expected. Figure 2 illustrates the effect of each treatment on water flux of the membrane. The permeability of raw membrane was computed to be 1.98 mL/cm^2/min/psi. The permeability decreased by 58% after sulfonation. An increase in $SO_3^-H^+$ group density decreased the permeability of the pure water. This is most likely due to the sulfonation reaction forming hydrogel in the pores that would constrict the membrane pores, thereby reducing the effective pore size. Similar results have been reported in literature where SEM micrographs have confirmed formation of hydrogels due to sulfonation of aryloxy or arylamino groups linked to polymers like phosphazenes.[45]

Sulfonation was followed by polymerization of styrene which resulted in further reduction of the permeability by 3.3 times. This is because polystyrene grafts were formed in the membrane flow path, reduced the effective pore size, and consequently decreased the permeability. Styrene polymerization was sequentially followed by ES polymerization. The decrease in permeability in this case was 1.5 times as compared to the styrene-grafted membrane. This is because the longer polymer grafts increased resistance to flow. A more substantial decrease was observed for poly(styrene-b-CMS)-grafted membranes to 0.03 mL/cm^2/min/psi (data not shown). The results are consistent with results reported by other researchers where they have observed a drop in permeability after functionalization showing evidence of polymer grafting.[9,18,46] It should be noted that the permeability of styrene-b-ES-grafted membrane is 0.16 mL/cm^2/min/psi which is higher than the permeability of a 30 kDa MWCO PES UF membrane (0.02 mL/cm^2/min/psi) based on the manufacturer reported test criteria. Therefore, although the pore size is reduced, these materials are still microfiltration membranes and are not plugged by formation of polymer grafts.

Characterization

Figure 3(a) shows the ^{1}H NMR spectrum of poly-CMS (PCMS) grafted in the pores of PES membrane. A sharp signal at $\delta = 1.57$ ppm is assigned to water. The peak at 1.7 and multiplets from 1.25 to 1.48 ppm represent the methine (—CH—) and methylene ($—CH_2—$) protons attached to the benzene ring, respectively.[47,48] Integration of the peaks yields a relative ratio of 1 : 2 which further confirms assignments of peaks to methine and methylene. The characteristic signal for the chloromethyl

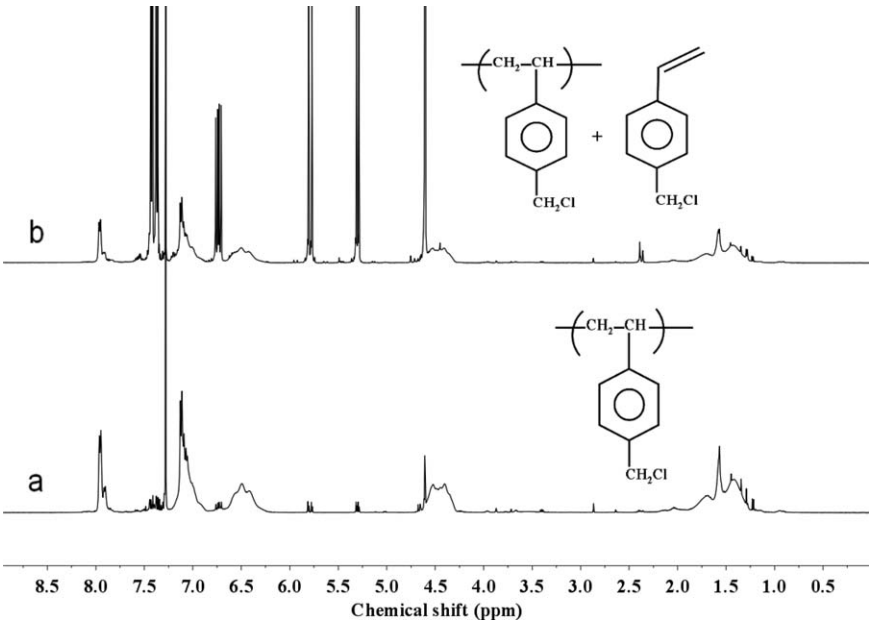

Figure 3. ^{1}H NMR spectra of (a) PCMS and (b) PCMS spiked with pure CMS.

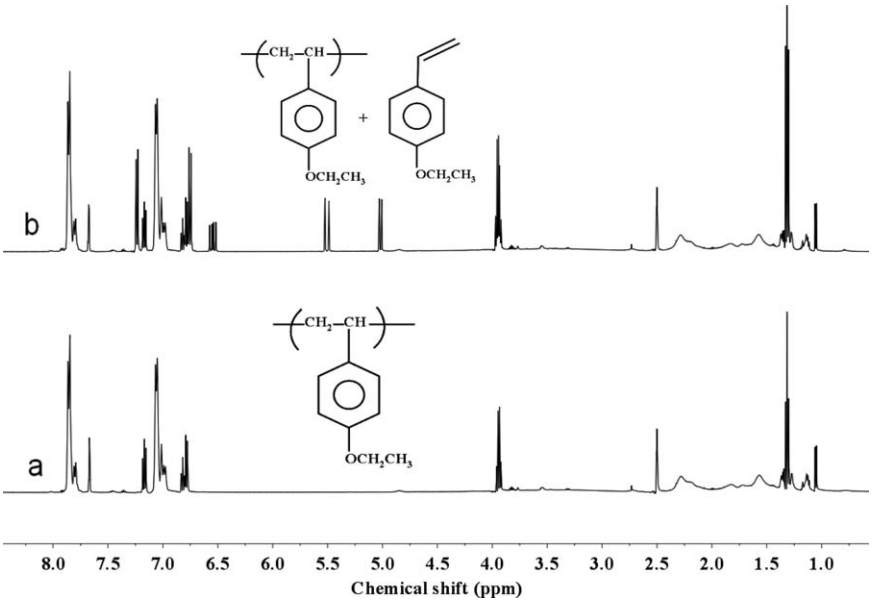

Figure 4. ^{1}H NMR spectra of (a) poly-ES and (b) poly-ES spiked with pure ES.

group can be seen at 4.5 ppm.[47,49,50] The integral value of peaks for chloromethyl group of CMS and PCMS is the same, indicating that the chloromethyl moiety is stable and has not undergone any side reactions. Peaks at 5.3, 5.8 (═CH), and 6.75 (═CH_2) are assigned to unreacted vinyl protons of the monomer (CMS).[49] However, by comparing the integral values, it was observed that these peaks make a very small contribution to the spectrum and hence can be neglected. This indicates that the double bond of the vinyl group (—CH═CH_2) is changed to single bond (—CH—CH_2—) after reaction with PES backbone. The multiple peaks between 7 and 8 ppm correspond to aromatic protons on the two phenyl rings of each PES repeat unit.[51,52] The signal at 7.28 ppm is from the solvent. The aromatic protons of pure CMS showed signal at 7.38 and 7.42. After polymerization reaction these protons were shifted to 6.4–6.8 with a broad signal, which is the characteristic of the polymer. Figure 3(b) shows the NMR spectrum of sample of PCMS spiked with pure monomer. The intensity of signals at 5.3, 5.8, and 6.75 which are the characteristic signal for protons on the vinyl backbone increases with addition of pure monomer. The intensity of aromatic protons of pure CMS at 7.38 and 7.42 also increases. This further gives the evidence that double bond of vinyl group is broken and PCMS is synthesized.

Figure 4(a) shows the NMR spectrum of poly-ES grafted in the pores of PES membrane. The quartet at 3.98 ppm is assigned to the —CH_2— protons of the ethoxy group (—OCH_2—CH_3). The triplet between 1.29 and 1.33 ppm is assigned to the —CH_3 protons of the ethoxy pendant group. The multiple peaks between 6.8 and 8 ppm is the characteristic of the protons on aromatic rings of poly-ES and PES repeating unit. The signal at 2.5 ppm is from the DMSO solvent. Figure 4(b) shows the NMR spectra of sample of poly-ES spiked with pure monomer. It can be seen that new peaks at 5, 5.5, and 6.5 appears on the spectrum. These peaks are characteristic of the protons on the vinyl backbone. The breaking of the double bond on the vinyl backbone causes these peaks to disappear in Figure 4(a), and peaks between 1 and 2.4 are assigned to protons on methine and methylene groups arising from cleavage of double bond.

Figures 5 and 6 show the NMR spectra of poly(styrene-b-ES) and poly(styrene-b-CMS), respectively. As seen during the formation of homopolymers, the chemical shift at 4.5 ppm is the characteristic of chloromethyl (—CH_2Cl) moiety on CMS monomer. The signal at 4.1 and 1.4 ppm is assigned to —CH_2— and —CH_3 group of ethoxy moiety. The broad signals from 6.4 to 8 ppm are from the aromatic protons on the polymers. The signals from 1.2 to 2.2 are from methine and methylene groups on the polymer backbone.

Quantification of Initiator Immoblization

The raw PES membrane was sulfonated to immobilize sulfonic acid groups as initiator for cationic polymerization. The sulfonic acid concentration was quantified by ion-exchange studies. IEC is the parameter that quantifies the number of ionizable groups in the membrane. IEC was determined in terms of milliequivalents of sodium ion exchanged per gram of membrane (dry weight).

The IEC of the raw membrane was determined experimentally to be 0.013 meq/g dry membrane. Ionizable groups are present due to mild surface modification performed by the manufacturer to improve membrane hydrophilicity. Sulfonated PES membrane has a maximum theoretical IEC of 0.32 meq/g. This value is based on an average pore size of 0.22 μm and 70% membrane porosity, yielding a total internal surface area of 30.75 m^2/g based on parallel, cylindrical pores with length equal to membrane thickness.[16] The IEC of the sulfonated membrane was experimentally determined to be 0.15 meq/g. This represents 46% of the maximum theoretical IEC. The higher IEC of the sulfonated membrane relative to the raw membrane was attributed to immobilized sulfonate groups in the membrane. The raw membrane represented <5% of the IEC of the

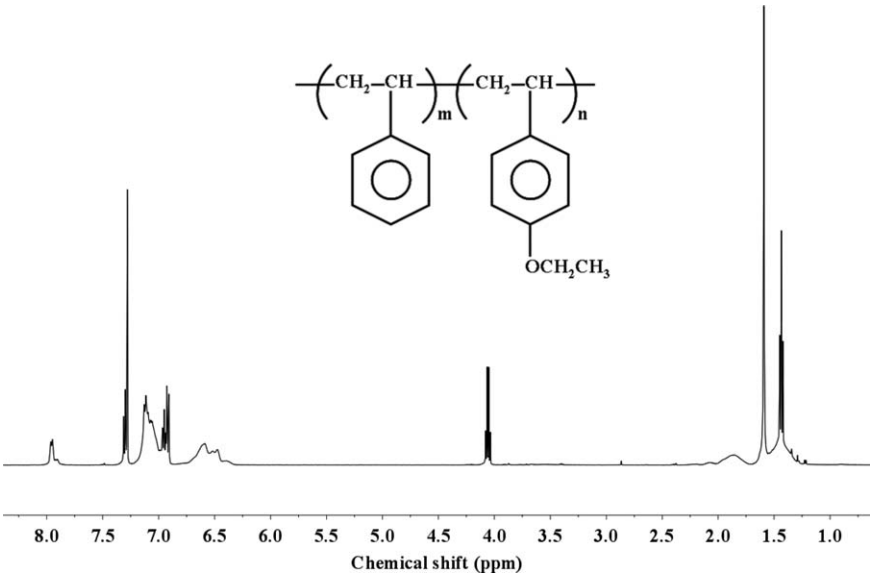

Figure 5. ^{1}H NMR spectra of poly(styrene-b-ES).

sulfonated membrane. In addition, the internal surface area was >99.9% of the total membrane area, and therefore sulfonate groups are mostly in the pores of the membrane and not on the external surface area. The results are consistent with work done by Ritchie and coworkers, who demonstrated successful introduction of sulfonic acid group onto PES.[16]

Styrene, CMS and ES Graft Quantification

Decreases in styrene and CMS concentrations, and thus retention in the membrane, were observed and quantified by decreases in the absorbance at the characteristic peaks of 291 and 295 nm, respectively, by UV–visible spectroscopy (UV–vis). It was observed that approximately 0.65 mmol of styrene and 0.4 mmol of CMS were retained on the membrane. Negligible decreases in absorbance were observed for either monomer when permeated through the raw membrane. This confirms that there was negligible graft formation in the pores of the membrane by cationic polymerization in the absence of initiator sulfonic acid groups. Additionally, when permeate samples were diluted in methanol to perform UV analysis, no precipitation or cloudiness was observed. This confirmed that the polystyrene did not come out and was retained in the pores of membrane.

The characteristic peak for ES by UV–vis was observed to be 283 nm. This was very close to the characteristic peak for toluene at 281 nm, and therefore, some amount of overlapping was seen on the spectrum. However, gas chromatography showed very clear and distinct separation between peaks for ES, toluene, and methanol. Consequently, the decrease in ES permeate concentration was quantified using gas chromatography at an elution time of 1.56 min which is far from methanol (0.1 min)

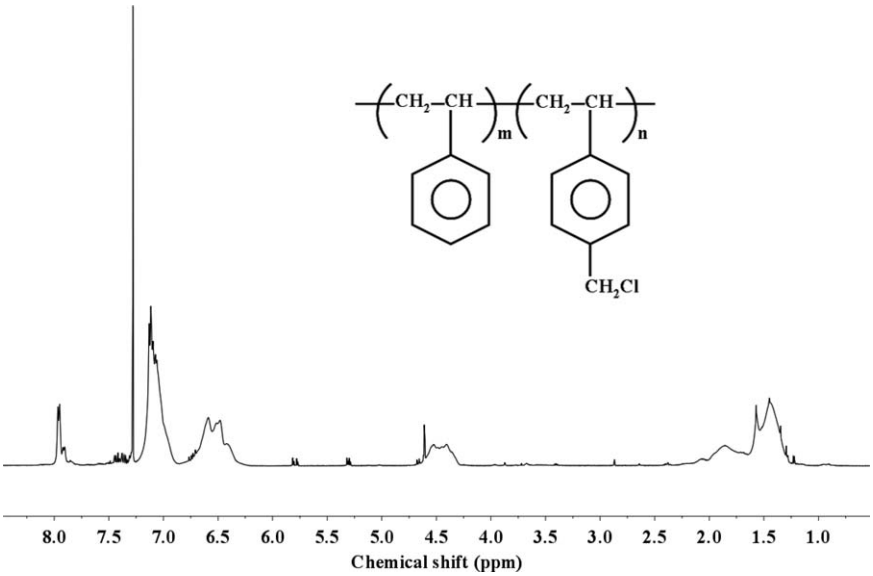

Figure 6. ^{1}H NMR spectra of poly(styrene-b-CMS).

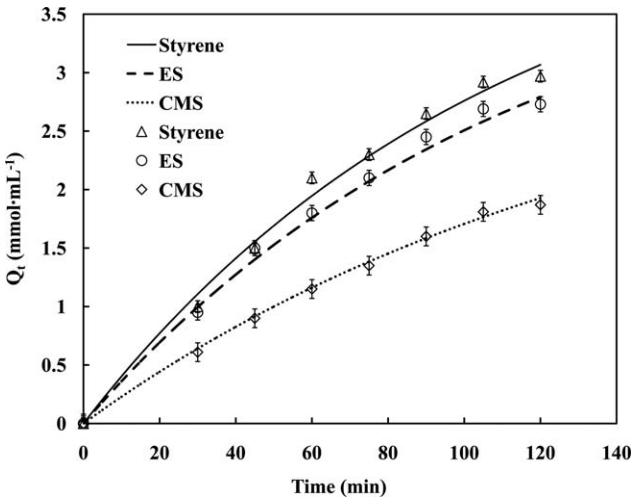

Figure 7. Kinetics of each monomer reacted. The smooth curves represent the pseudo-first-order equation fit and the data points represent experimental observations.

and toluene (0.2 min). It was observed that 0.52 mmol of ES was retained on the membrane.

Kinetics of Each Monomer Reacted

The amount of monomer retained on the membrane was measured at definite intervals of time over 120 min. The membrane volume was calculated to be 0.21 mL based on an effective diameter of 4.1 cm and a thickness of 160 μm. Concentration was measured in terms of mmol of styrene reacted per milliliter of membrane. Concentration was plotted versus time as shown in Figure 7. It was observed that reaction of monomer was initially rapid and then gradually slowed down. This is most likely due to initial availability of active sites for polymerization. The growing grafts form a diffusion barrier that gradually slows down the reaction rate.

The reaction rate order was determined to be best approximated as pseudo-first-order. There are several reasons why pseudo-first-order rate kinetics are a good fit for cationic polymerization of styrene and modified styrenes in a membrane. First, the initiator is provided by sulfonic acid groups on the pore walls, and these are associated with the growing ends of the polymer grafts. Second, cationic polymerization is a living polymerization, so the concentration of the propagating species is constant. Finally, a second-order rate expression was a poor fit of the kinetic data; by contrast, pseudo-first order kinetics provided an excellent fit.

The pseudo-first-order kinetic expression shown in eq. (1) was used to model the experimental data,

$$Q_t = Q_e(1-e^{-kt}) \quad (1)$$

where Q_e and Q_t (mmol·mL^{-1}) are the amounts of monomer retained on the membrane at equilibrium and at time t (min), respectively, and k (min^{-1}) is the pseudo-first-order rate constant. The parameter Q_e was treated as an adjustable parameter in the above expression, and was determined by performing regression analysis using the method of least squares to best fit the model with experimental data. The linearized form of eq. (1) is shown in Table I. The values of the rate constant, k, were determined from the slope of the straight line obtained by plotting $\ln(Q_e - Q_t)$ versus t. The values of k, Q_e, and correlation coefficients (R^2) are shown in Table I.

It was observed from the R^2 values and Figure 7 that the model correlates well with the experimental data. By comparing the rate constants for different monomers, it was observed that styrene and ES reacted approximately at the same rate while CMS reacted nearly 25% slower than styrene and ES. Furthermore, the slope between 100 and 120 min is still positive and not showing a plateau. This indicates that although the rate is gradually slowing down, the amount of monomer retained on membrane has not reached a maximum value and may increase if reaction is carried out beyond 120 min. This result is correlated with the model which shows a computed value of Q_e greater than predicted at 120 min of polymerization reaction time. Hence, the model holds well until 120 min of polymerization reaction time. However, the validity of the model needs to be investigated for reaction times beyond 120 min.

The amounts of monomer reacted each for styrene, ES, and CMS were 2.97, 2.73, and 1.87 mmol·mL^{-1}, respectively, at 120 min of reaction time. This indicated that CMS is the least reactive and styrene and ES showed approximately similar reactivity. The low reactivity of CMS is due to the strong electron-withdrawing chloromethyl substituent. Chlorine is highly electronegative and moves electron density away from the ring due to the negative inductive effects. The presence of an electron-withdrawing substituent inhibits the reactivity of monomer because cationic polymerization is limited to electron-donor substituents. Alkoxy group is an electron donor because the alkyl group is an electron donor. Additionally, one of the two lone pairs of electrons on the oxygen forms a pi orbital overlap (resonance effect) which gives the oxygen an overall positive charge pushing the monomer toward the negatively charged initiator. Therefore, the higher reactivity of ES relative to CMS was reasonable. The results are consistent with those reported by Kamigaito and co-workers.[48] In their work, CMS showed low

Table I. Pseudo-First-Order Model Parameters

$\ln(Q_e - Q_t) = \ln Q_e - kt$			
Monomer	k (min^{-1})	Q_e (mmol·mL^{-1})	R^2
Homopolymers			
Styrene	0.0092	4.6	0.9883
ES	0.0088	4.3	0.9914
CMS	0.0069	3.4	0.9974
Block copolymers			
Poly (styrene-co-CMS)	0.0059	2.2	0.9968
Poly (styrene-co-ES)	0.0075	3.8	0.9929
Different monomer feed concentration			
5 vol % styrene	0.0092	4.6	0.9883
10 vol % styrene	0.020	5.6	0.9613
15 vol % styrene	0.024	9	0.9721

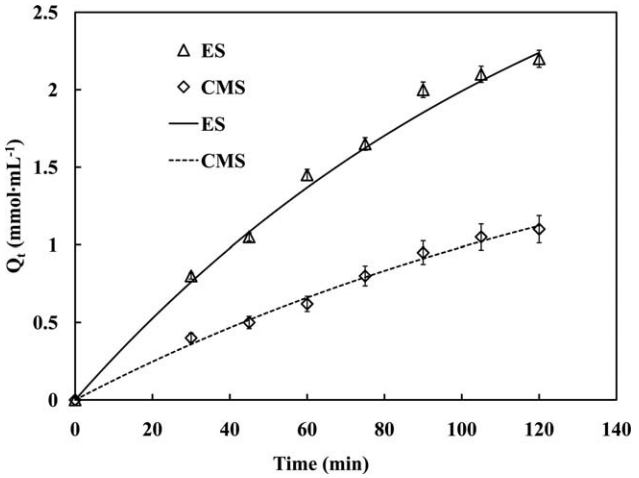

Figure 8. Kinetics of CMS and ES reacted after polymerization with styrene. The smooth curves represent the pseudo-first-order equation fits and the data points represent the experimental observation.

reactivity relative to styrene during homopolymerization and copolymerization by cationic polymerization using alcohol as an initiator and boron trifluoride etherate as an activator. Their work also showed that methoxy styrene was more reactive than CMS. This confirms that a monomer with an electron-donor group (alkoxy) is more reactive than a monomer with an electron-withdrawing group (chloromethyl).

Kinetics of CMS/ES During Formation of Block Copolymer Grafts

Figure 8 shows the amounts of CMS and ES retained on the membrane after polymerization with styrene. The pseudo-first-order rate expression discussed in the section entitled "Kinetics of Each Monomer Reacted" was used to model the experimental data. Correlation coefficients show reasonably good fits of the experimental data with the model. The values of k are reported in Table I and indicate that formation of styrene-b-ES block copolymer was roughly 1.25 times faster than styrene-b-CMS block copolymer. The amounts of CMS and ES retained on the membrane during formation of block copolymer were 60 and 80%, respectively, of the amount retained during formation of homopolymer. This was most likely due to lower site accessibility because of the diffusion barrier caused by the already present styrene grafts.

Controlled Polymer Growth

In this study, controlled growth of styrene polymer was evaluated through the variation of reaction parameters like monomer feed concentration and initiator reaction time. The study aimed to build an understanding of the process of polymer growth and the reaction mechanism so that data could be used in the future for further optimization of specific applications like antibody adsorption. The kinetics of polymer growth, average graft length, and IEC were evaluated as a function of these reaction parameters.

Kinetics. Styrene reaction kinetics was studied for different feed concentrations. A plot of styrene retained versus time is shown in Figure 9. The pseudo-first-order rate expression (eq. (1)) was used to fit the experimental data. The values of k, Q_e, and R^2 were obtained by the same method as described in the section entitled "Kinetics of Each Monomer Reacted", and are reported in Table I. It can be observed that experimental data matches reasonably well with the model equation. The reaction proceeds rapidly and then gradually slows down. However, it should be noted that it did not show a plateau within 120 min of polymerization reaction time. It was observed from experimental data that the amount of monomer retained on the membrane at 120 min of reaction time increased approximately linearly with monomer feed concentration. By comparing the value of rate constants, it was observed that the rate of reaction for 15% monomer feed concentration was roughly 2.6 and 1.2 times higher than 5 and 10% feed concentration, respectively. Furthermore, it was observed that the value of Q_e almost doubled as the monomer feed concentration increased from 5 to 15%. This indicated that a higher feed monomer concentration increased the driving force for mass transfer through the grafts.

The amount of styrene retained was also measured and plotted for different initiator reaction times. Monomer feed concentrations were kept constant at 5 vol % and the polymerization reaction time was 120 min. It can be seen from Figure 10 that the grafting level increased sharply with increase in initiator reaction time from 45 to 135 min. This is because with increase in sulfonation reaction time, more active sites are available for polymerization. After approximately 135 min, however, there is no significant increase in the percentage of styrene retained. This is because number of initiator sites reached a maximum, and the polymerization rate reached a corresponding peak.

Graft Length. Data in the previous section showed how the monomer and initiator concentrations affect monomer retention in the membrane. The monomer was retained as polymer grafts were formed in the pores. One way to characterize grafted chains is by calculating an average graft length, similar to an average degree of polymerization. The average graft length was determined as a ratio of the moles of monomer retained

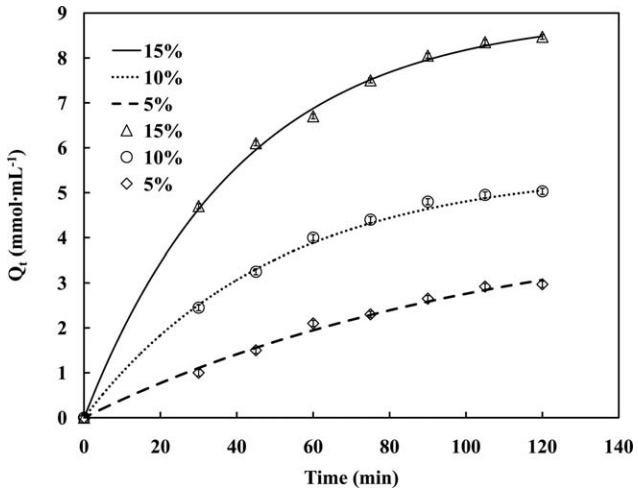

Figure 9. Kinetics of styrene reacted for different feed concentration. The smooth curves represent the fit with pseudo-first-order equation and the data points represent the experimental observation.

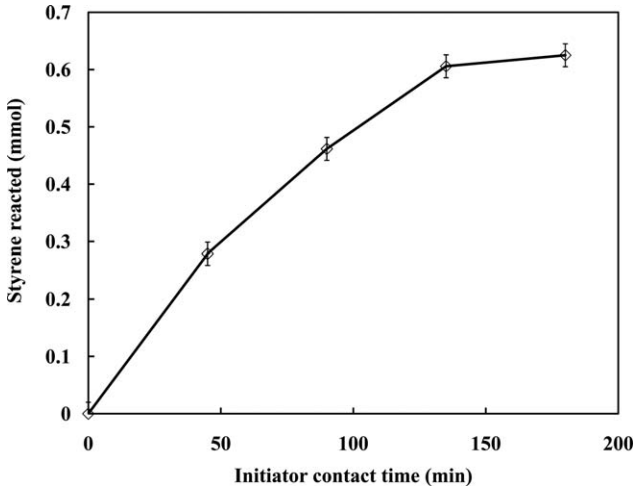

Figure 10. Effect of initiator reaction time on amount of styrene reacted.

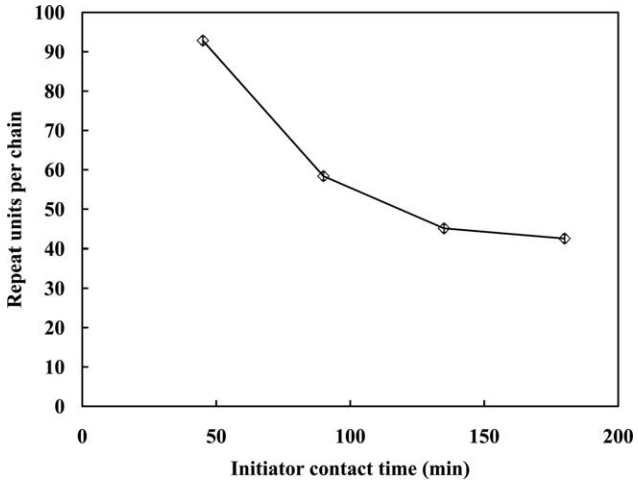

Figure 12. Effect of initiator reaction time on graft length.

divided by the moles of initiator sites in the membrane. The moles of monomer retained was determined from a material balance on the monomer reaction permeate solution. The number of initiator sites available for reaction was determined from ion exchange of sulfonic acid with sodium ions on a one-to-one basis. For example, the average graft length would increase for membranes with the same initiator contact time, but with increasing monomer concentrations during graft synthesis as in Figure 11.

Graft length was determined assuming that all the styrene retained on the membrane undergoes polymerization and that unreacted styrene remains in the permeate. The assumption was justified because reacted styrene becomes part of the carbocation that interacts with the immobilized initiator (sulfonic acid groups). Also there was no evidence of styrene monomer absorption by the membrane. The bulk of the polymer grafts were formed in the membrane pores because the external surface area is 0.1% of total available area. As illustrated in Figure 11, it was observed that the number of repeat units per graft was a linear function of monomer feed concentration. The polymerization reaction time was 120 min. Polymer grafts with as many as 125 repeat units per chain were grafted with 15% monomer concentration in the feed. However, it should be noted here that significant membrane swelling and cracking was observed for a feed concentration of 20% monomer.

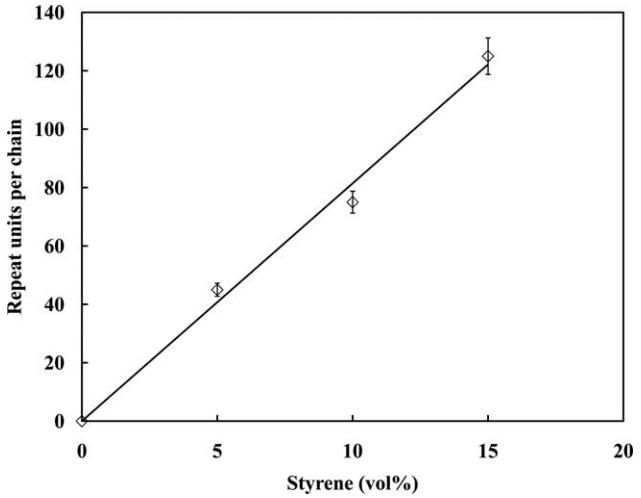

Figure 11. Influence of monomer feed concentration on graft length. Polymerization reaction time was 120 min.

There was evidence of steric hindrance and crowding effects as the initiator concentration was increased. The data in Figure 12 showed how graft length changed with increasing initiator reaction time. The monomer concentration was held constant at 5% and the polymerization time was 120 min. The data showed a rapid change from long grafts at low initiator contact time to shorter grafts at higher initiator contact time. The chain length did reach a uniform average length at longer times because there was no increase in the number of initiator sites. The reduction in graft length was most likely due to steric hindrance caused by higher initiator surface density, where all active sites are not accessible at higher contact time. This also indicated that polymer growth was constant above a critical initiator surface density. This was confirmed by normalizing the data shown in Figure 10, where there was no significant change in amount of styrene retained after 135 min of initiator contact time.

Ion-Exchange Capacity. The functionalized membrane was also characterized by ion-exchange capacity to quantify changes to the membrane. The membrane was first sulfonated at different initiator contact times. For each contact time, the membrane was polymerized to form polystyrene grafts. After polymerization, the membrane was again sulfonated prior to measuring the IEC of the grafted membrane. Figure 13 shows the effect of initiator contact time on IEC (meq/g) of the grafted membrane. The polymerization reaction time was 120 min for all three monomer concentrations. It can be seen that the IEC value increased with increasing initiator contact time for all three monomer concentrations. For lower initiator contact time (50 and 100 min), the IEC increased linearly with increased monomer concentration. After 135 min of initiator reaction time, the IEC approached a maximum where the initiator sites were saturated and no further change in IEC was observed. Thus, at lower initiator reaction times, fewer grafts were formed and IEC was lower. At higher initiator contact times, the number of

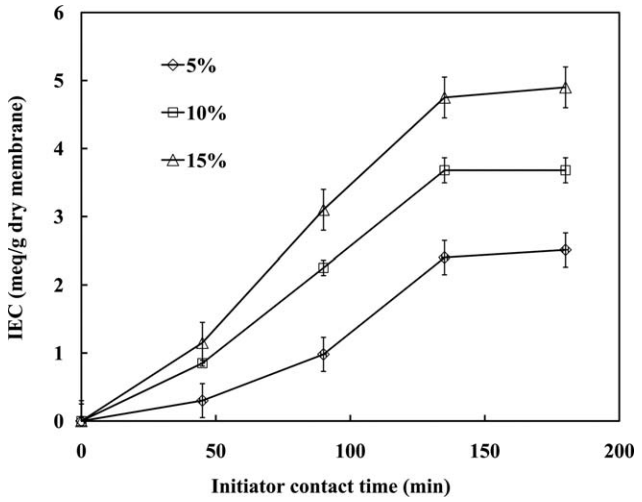

Figure 13. Effect of initiator reaction time and monomer feed concentration on IEC.

initiator sites available for grafting was higher, more grafts were formed and the IEC was higher. The IEC value was highest (4.9 meq/g) for 15% monomer concentration and 135 min of initiator reaction time. This corresponds to more than 350 times greater IEC than raw membrane and approximately 18 times greater than sulfonated membrane. The IEC stayed constant for initiator contact time greater than 135 min but it still showed linear dependency for change in monomer feed concentration. This indicated that both the reaction parameters have significant influence on IEC at lower initiator contact times. However, at higher initiator contact times, change in monomer feed concentration dominated and had a more profound effect on IEC.

CONCLUSIONS

A novel polymeric, functionalized membrane has been created by cationic polymerization of styrene and substituted styrene monomers. Homopolymer and block copolymer grafts have been synthesized in the pores of microfiltration PES membrane. The quantitative information from the analytical experiments and material balances showed that the membrane has a very high IEC of (4.9 meq/g) with roughly 125 repeat units per chain. This represents roughly 92% of theoretical maximum (5.3 meq/g) IEC of an ion-exchange resin. Synthesis of homopolymer and block copolymer grafts has been confirmed by UV–visible spectroscopy and gas chromatography analysis of the feed and permeate solutions. Permeability studies at each step were performed. The results revealed that there is an order of magnitude decrease in pure water permeability from raw to sulfonated to styrene-grafted and finally styrene-b-ES-grafted membrane. This result further confirmed the presence of grafted polymer in the membrane.

The kinetics of reaction of each monomer during formation of homopolymer grafts were studied. Pseudo-first-order kinetic expression correlated well with the experimental data for each monomer reacted. It was observed that CMS was the least reactive and styrene and ES showed similar reactivity during formation of homopolymer. CMS reacted approximately 25% slower as compared to styrene and ES. The low reactivity of CMS is due to the presence of a strong electron-withdrawing chloromethyl pendant group. Ethoxy moiety in the ES monomer has an electron-donor substituent which makes it more reactive relative to CMS. Similar observations were reported during formation of block copolymers poly(styrene-b-CMS) and poly(styrene-b-ES). CMS reacted approximately 22% slower than ES after polymerization with styrene. ES and CMS showed low reactivity during formation of block copolymer as opposed to during formation of homopolymer. This is due to the diffusion barrier by polystyrene grafts already present in the pores of membrane.

Finally, controlled polymer growth of styrene monomer was studied to understand the process and control of the polymerization reactions. This was done by studying the effects of monomer concentration and initiator reaction time on polymer growth aspects like kinetics, amount of styrene reacted, IEC, and graft length. At lower initiator surface density, graft length and IEC were impacted by both monomer feed concentration and initiator contact time. However, for higher initiator surface density, the monomer feed concentration parameter dominates.

ACKNOWLEDGMENTS

We gratefully acknowledge the financial support provided by the National Science Foundation under NSF Award Number CBET-0756460. We also thank Dr. Ken Belmore (NMR facility manager, The University of Alabama) for help in performing the NMR analysis.

REFERENCES

1. Causserand, C.; Lebleu, N.; Roques, C.; Aimar, P. *J. Membr. Sci.* **2009**, *326*, 178.
2. van Reis, R.; Zydney, A. *Curr. Opin. Biotech.* **2001**, *12*, 208.
3. Urkiaga, A.; De las Fuentes, L.; Acilu, M.; Uriarte, J. *Desalination* **2002**, *148*, 115.
4. Vaillant, F.; Millan, A.; Dornier, M.; Decloux, M.; Reynes, M. *J. Food Eng.* **2001**, *48*, 83.
5. Vial, D.; Doussau, G. *Desalination* **2003**, *153*, 141.
6. Ezzati, A.; Gorouhi, E.; Mohammadi, T. *Desalination* **2005**, *185*, 371.
7. Ritchie, S. M. C.; Kissick, K. E.; Bachas, L. G.; Sikdar, S. K.; Parikh, C.; Bhattacharyya, D. *Environ. Sci. Technol.* **2001**, *35*, 3252.
8. Bhattacharyya, D.; Datta, S.; Cecil, C. *Ind. Eng. Chem. Res.* **2008**, *47*, 4586.
9. Ritchie, S. M. C.; Bachas, L. G.; Olin, T.; Sikdar, S. K.; Bhattacharyya, D. *Langmuir* **1999**, *15*, 6346.
10. Datta, S.; Ray, P. D.; Nath, A.; Bhattacharyya, D. *J. Membr. Sci.* **2006**, *280*, 298.
11. Smuleac, V.; Butterfield, D. A.; Sikdar, S. K.; Varma, R. S.; Bhattacharyya, D. *J. Membr. Sci.* **2005**, *251*, 169.
12. Ladhe, A. R.; Xu, J.; Hollman, A. M.; Smuleac, V.; Bhattacharyya, D. In Comprehensive Membrane Science and

Engineering; Editor-in-Chief: Enrico, D.; Lidietta, G.; Eds.; Elsevier Science: Oxford, **2010**; Vol. *1*, Chap. 1.02, pp 13.

13. Zydney, A. L.; van Reis, R. *Comprehensive Biotechnology (Second Edition)*. **2011**, *5*, 499.
14. Hestekin, J. A.; Bachas, L. G.; Bhattacharyya, D. *Ind. Eng. Chem. Res.* **2001**, *40*, 2668.
15. Ladhe, A. R.; Xu, J.; Hollman, A. M.; Smuleac, V.; Bhattacharyya, D. In Comprehensive Membrane Science and Engineering; E. Drioli; L. Giorno, Eds.; Elsevier: New York, **2010**, pp 13.
16. Shah, T. N.; Goodwin, J. C.; Ritchie, S. M. C. *J. Membr. Sci.* **2005**, *251*, 81.
17. Shah, T. N.; Ritchie, S. M. C. *Appl. Catal. A-Gen.* **2005**, *296*, 12.
18. Cowan, S.; Ritchie, S. *Separ. Sci. Technol.* **2007**, *42*, 2405.
19. Bhattacharya, A.; Misra, B. N. *Prog. Polym. Sci.* **2004**, *29*, 767.
20. Ladhe, A. R.; Radomyselski, A.; Bhattacharyya, D. *Langmuir* **2006**, *22*, 615.
21. Bhattacharyya, D.; Hestekin, J. A.; Brushaber, P.; Cullen, L.; Bachas, L. G.; Sikdar, S. K. *J. Membr. Sci.* **1998**, *141*, 121.
22. Baker, A. R.; Fournier, R. L.; Sarver, J. G.; Long, J. L.; Goldblatt, P. J.; Horner, J. M.; Selman, S. H. *Cell Transplant.* **1997**, *6*, 585.
23. Ito, Y.; Inaba, M.; Chung, D. J.; Imanishi, Y. *Macromolecules* **1992**, *25*, 7313.
24. Kai, T.; Tsuru, T.; Nakao, S.; Kimura, S. *J. Membr. Sci.* **2000**, *170*, 61.
25. Kim, J. H.; Ha, S. Y.; Nam, S. Y.; Rhim, J. W.; Baek, K. H.; Lee, Y. M. *J. Membr. Sci.* **2001**, *186*, 97.
26. Yamaguchi, T.; Nakao, S.; Kimura, S. *Macromolecules* **1991**, *24*, 5522.
27. Choi, Y. J.; Yamaguchi, T.; Nakao, S. *Ind. Eng. Chem. Res.* **2000**, *39*, 2491.
28. Yanagioka, M.; Kurita, H.; Yamaguchi, T.; Nakao, S. *Ind. Eng. Chem. Res.* **2003**, *42*, 380.
29. Hautojarvi, J.; Kontturi, K.; Nasman, J. H.; Svarfvar, B. L.; Viinikka, P.; Vuoristo, M. *Ind. Eng. Chem. Res.* **1996**, *35*, 450.
30. Hollman, A. M.; Bhattacharyya, D. *Langmuir* **2002**, *18*, 5946.
31. Ritchie, S. M. C. In New Insights into Membrane Science and Technology: Polymeric and Biofunctional Membranes; 1st ed.; D. Bhattacharyya; Butterfield, D. A.; Eds.; Elsevier: New York, **2003**, Chap. 15, pp 299.
32. Hollman, A. M.; Bhattacharyya, D. In New Insights into Membrane Science and Technology: Polymeric and Biofunctional Membranes; D. Bhattacharyya; Butterfield, D. A.; Eds.; Elsevier: Amsterdam, **2003**, pp 329.
33. Cohen, Y.; Lewis, G. T.; Nguyen, V. *J. Polym. Sci. Pol. Chem.* **2007**, *45*, 5748.
34. Braunecker, W. A.; Matyjaszewski, K. *Prog. Polym. Sci.* **2007**, *32*, 93.
35. Singh, N.; Husson, S. M.; Zdyrko, B.; Luzinov, I. *J. Membr. Sci.* **2005**, *262*, 81.
36. Singh, N.; Wang, J.; Ulbricht, M.; Wickramasinghe, S. R.; Husson, S. M. *J. Membr. Sci.* **2008**, *309*, 64.
37. Wandera, D.; Wickramasinghe, S. R.; Husson, S. M. *J. Membr. Sci.* **2011**, *373*, 178.
38. Friebe, A.; Ulbricht, M. *Langmuir* **2007**, *23*, 10316.
39. Yang, Q. A.; Ulbricht, M. *Macromolecules* **2011**, *44*, 1303.
40. Mueller, L.; Matyjaszewski, K. *Macromol. React. Eng.* **2010**, *4*, 180.
41. Trapa, P. E.; Huang, B. Y.; Won, Y. Y.; Sadoway, D. R.; Mayes, A. M. *Electrochem. Solid St.* **2002**, *5*, A85.
42. Pandey, A. K.; Goswami, A.; Sen, D.; Mazumder, S.; Childs, R. F. *J. Membr. Sci.* **2003**, *217*, 117.
43. Xu, T. W. *J. Membr. Sci.* **2005**, *263*, 1.
44. Matyjaszewski, K. Cationic polymerizations: mechanisms, synthesis, and applications; Marcel Dekker: New York, **1996**.
45. Allcock, H. R.; Fitzpatrick, R. J.; Salvati, L. *Chem. Mater.* **1991**, *3*, 1120.
46. Hollman, A. M.; Scherrer, N. T.; Cammers-Goodwin, A.; Bhattacharyya, D. *J. Membr. Sci.* **2004**, *239*, 65.
47. Li, Q. Y.; Wu, Y. X.; Ma, W. Y.; Xu, R. W.; Wu, G. Y.; Yang, W. T. *Chinese J. Polym. Sci.* **2010**, *28*, 449.
48. Kamigaito, M.; Nakashima, J.; Satoh, K.; Sawamoto, M. *Macromolecules* **2003**, *36*, 3540.
49. Shin, J.; Fei, G.; Kang, S. A.; Ko, B. S.; Kang, P. H.; Nho, Y. C. *J. Appl. Polym. Sci.* **2009**, *113*, 2858.
50. Goh, Y. T.; Patel, R.; Im, S. J.; Kim, J. H.; Min, B. R. *Korean J. Chem. Eng.* **2009**, *26*, 518.
51. Lu, D. P.; Zou, H.; Guan, R.; Dai, H.; Lu, L. *Polym. Bull.* **2005**, *54*, 21.
52. Klaysom, C.; Ladewig, B. P.; Lu, G. Q. M.; Wang, L. Z. *J. Membr. Sci.* **2011**, *368*, 48.